(A New Proposal to Jefferson Lab PAC18) Measurement of neutron (^{3}He) spin structure functions in the resonance region.

D. Margaziotis
California State University, Los Angeles, CA 90032

J.-C. Yang
Chungnam National University, Taejon, Korea

A. Deur, Y. Roblin
University Blaise Pascal, Clermont-Ferrand, France

L. Kramer, P. Markowitz
Florida International University and Jefferson Lab

J.R.M. Annand, D.G. Ireland, J.D. Kellie, K. Livingston, G. Rosner, D.P. Watts
University of Glasgow, Glasgow G12 8QQ, Scotland, UK

R. De Leo
INFN-Bari, Italy

F. Cusanno
INFN-Sanita, Italy

S. Frullani, F. Garibaldi, M. Iodice, R. Iommi, G. Urciuoli
INFN-Roma, Italy

J. P. Chen (Spokesperson), E. Chudakov, R. Ent, J. Gomez, J.-O. Hansen, K. de Jager, M. Kuss, N. Liyanage (Spokesperson and contact person) J. LeRose, R. Michaels, J. Mitchell, A. Saha, B. Wojtsekhowski
Jefferson Lab, Newport News, VA 23606

A.T.Katramatou, G. G. Petratos
Kent State University, Kent, OH 44242

D. Dale, W. Korsch P. Zolnierczuk
University of Kentucky, Lexington, KY 40506

G. Chang, J. Kelly
University of Maryland, College Park, MD 20742

W. Berttozi, C. Crawford, D. Dutta, H. Gao, S. Gilad, D. Higinbotham, S. Sirca, R. Suleiman, H. Xiang, F. Xiong, W. Xu, Z. Zhou, L.Y. Zhu
Massachusetts Institute of Technology, Cambridge, MA 02139

L. Kaufman, K. Kumar
University of Massachusetts, Amherst, MA 01003

F. W. Hersman
University of New Hampshire, Durham, NH 03824

V. Punjabi
Norfolk State University, Norfolk, VA 23504

L. Todor, L. Weinstein
Old Dominion University, Norfolk, VA 23508

G. Cates, B. Humensky, I. Kominis
Princeton University, Princeton, NJ 08544

E. Brash
University of Regina, Regina, SK, S4S OA2, Canada

S. Dieterich, R. Gilman, C. Glashausser, X. Jiang, G. Kumbartzki,
R. Ransome, S. Strauch
Rutgers University, Piscataway, NJ 08855

L. Auerbach, S. Choi (Spokesperson), Z.-E. Meziani, K. Slifer
Temple University, Philadelphia, PA 19122

H. Tsubota
Tohoku University, Sendai, Japan

D. Armstrong, D. T. Averett, P. Djawotho, M. Finn, K. Griffioen, K. Kramer
College of William and Mary, Williamsburg, VA 23185

June 1, 2000

Abstract

We propose a precision extraction of the neutron spin structure function g_1^n and the virtual photon asymmetry A_1^n in the resonance region over a moderate Q^2 range (up to $Q^2 = 4.2(GeV/c)^2$) using a polarized ^{3}He target. The Bloom-Gilman duality has been experimentally demonstrated for the spin independent structure functions down to small values of Q^2. The proposed experiment combined with Deep-Inelastic-Scattering data will provide a precision test of quark-hadron duality predictions for spin structure functions. The demonstration of duality for spin structure functions will enable the use of resonance data as a powerful tool to study the nucleon spin structure in the very high x region.

1 Introduction

We are proposing a precision extraction of neutron spin structure function g_1 and the virtual photon asymmetry A_1 in the resonance region using the Hall A polarized ^{3}He target. The quantities g_1 and A_1 carry valuable information about the spin of the parton distributions that make up the nucleon. At low values of x, g_1 and A_1 are sensitive to the sea of $q\bar{q}$ pairs whereas at high x they can be used to study the valence quark spin structure.

A large amount of spin structure data [1] in the Deep Inelastic Scattering (DIS) region has become available over the last two decades. The precision of DIS spin structure data continues to improve with advancements in polarized beam and polarized target technologies. However, very little spin structure data are available in the resonance region. This is especially true for the neutron. Due to the lack of a free neutron target, experiments have been performed with polarized deuteron and ^{3}He targets to extract neutron spin information. Using a polarized deuteron target SLAC experiment E-143 [2] extracted neutron spin structure functions (SSF) in the resonance region for $Q^2 < 1.2$ (GeV/c)^2. Jefferson lab experiment E94-010 [3] used a polarized ^{3}He target to do a high precision extraction of resonance spin structure functions for the neutron for $Q^2 < 1.0$ (GeV/c)^2. The results from this experiment are expected soon. However, in the moderate Q^2 region of $1.5 < Q^2 < 10$ (GeV/c)^2, there is no SSF data in the resonance region available at present. Some neutron SSF data in the resonance region are expected to become available in the near future from two Jefferson Lab experiments [4]. Both these experiments will be using polarized ND_3 targets to extract neutron information. This proposal discusses a high precision extraction of the neutron spin structure functions g_1 and the virtual photon asymmetry A_1^n in the resonance region using a polarized ^{3}He target as an effective neutron target. These data will be complementary to the neutron data extracted using polarized ND_3 targets in Halls B and C. These data combined with the precision high x spin structure function data in the DIS region from experiment 99-117 [5] can be used for a stringent test of quark-hadron duality for spin structure functions.

Thirty years ago Bloom and Gilman [6] made the observation that the scaling curve seen at high momentum transfer is an accurate average over the resonance bumps at lower momentum transfer but at the same value of x. This duality between the resonance region, which is best described by constituent quark models, and the scaling region, which is governed by PQCD, hints a common origin for the both regions. Several years after the observation of duality, De Rujula, Georgi and Politzer [7] suggested a framework based on the QCD operator product expansion (OPE) within which the averaging of the resonance bumps to the scaling curve can be interpreted in terms of the role of higher twists in DIS. Following the OPE they showed that at moderate values of Q^2 the higher twist corrections to the lower moments of the structure functions are small while the corrections to higher moments are large. Thus, at moderate values of Q^2, the value of a structure function averaged over a sufficiently wide interval of energy cannot be much different from its value at high Q^2. However, due to large corrections to higher moments, at a given energy the difference can be significant. More recently Carlson and Mukhopadhyay [8] have done a further QCD analysis of duality that includes the treatment of background under the resonance peaks. Ji and Unrau [9] have also examined QCD implications of duality. As one of the applications of duality, Ji

and Melnitchouk [10] illustrated that higher twist matrix elements could be extracted from resonance data. Recent data from Jefferson Lab Hall C [11] have further confirmed that Bloom-Gilman duality holds to a few percent level down to small values of Q^2. The striking agreement shown by this data for unpolarized structure functions between the resonance and the scaling regions indicates that it is reasonable to expect duality for polarized structure functions as well. Recently Carlson and Mukhopadhyay [12] have predicted quark-hadron duality for Spin Structure Functions.

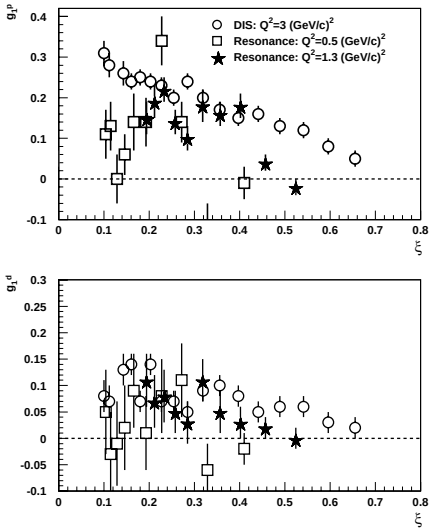

Figure 1: g_1^p and g_1^d measured by SLAC experiment E143 [2] in DIS and resonance regions.

Figure 1 shows g_1^p and g_1^d measured by SLAC experiment E143 [2] in DIS and resonance regions plotted as a function of the Nachtmann scaling variable $\xi = 2x/(1+\sqrt{1+4M^2x^2/Q^2})$. For the case of the proton the g_1 resonance data at very low Q^2 ($Q^2 = 0.5$ (GeV/c)^2) differ significantly from g_1 data measured in the DIS region. For the $Q^2 = 1.2$ (GeV/c)^2 case the the resonance data seem to approach the DIS data indicating the possible onset of duality. It is not possible to draw any conclusion about the g_1^n in DIS and resonance regions because of the large statistical uncertainties for the deuteron measurement. Hall A experiment E94-010 [3] data is expected to produce g_1^n with high statistical accuracy for $Q^2 < 1.2$ (GeV/c)^2. The measurement we are proposing here will allow us to extend this data to $Q^2 < 4.3$ (GeV/c)^2.

While it is interesting in its own right to test duality predictions for spin structure functions, such a test can lead to very important applications. The measurement of the spin structure functions and the virtual photon asymmetry (A_1) remains crucial to the understanding of the valence quark structure of the nucleon. Different theories and models provide dramatically different predictions for $A_1^{n,p}$ in the high x region. Exact SU(6) symmetry requires that $A_1^n = 0$ and $A_1^p = 5/9$. Quark models with broken SU(6) symmetry predict that both $A_1^p \to 1$ and $A_1^n \to 1$ as $x \to 1$ [13] [14] [15]. PQCD calculations [16] [17] also show that

$A_1^p \to 1$ and $A_1^n \to 1$ as $x \to 1$. A recent approach [18] that uses instantons as an important degree of freedom predicts that A_1^n remains negative or close to zero.

Although much more spin structure data exist for the DIS region than for the resonance region, most of these data are limited to the lower x region. This is mainly due to kinematic restrictions in the DIS region that make it difficult to access the high x region. As shown in Figures 2 and 3, this situation is even worse for the neutron due to lack of a free neutron target. Jefferson lab experiment 99-117 intends to measure A_1^n in the DIS region up to $x = 0.63$ with high precision. The availability of 12 GeV beam at Jefferson lab would allow extending this measurement to $x = 0.75$. However, kinematic constraints make it almost impossible to measure A_1^n and spin structure functions in the DIS region above $x \approx 0.75$. These kinematic restrictions do not apply to the resonance region data. With the availability of 12 GeV beam, it will be relatively easy to measure A_1 and g_1 in the resonance region up to x values as high as 0.95. Therefore if duality is established between the resonance region and the DIS region in the overlap range of $x < 0.75$, the resonance data can be used as a very powerful tool to infer the DIS behavior up to very high values of x.

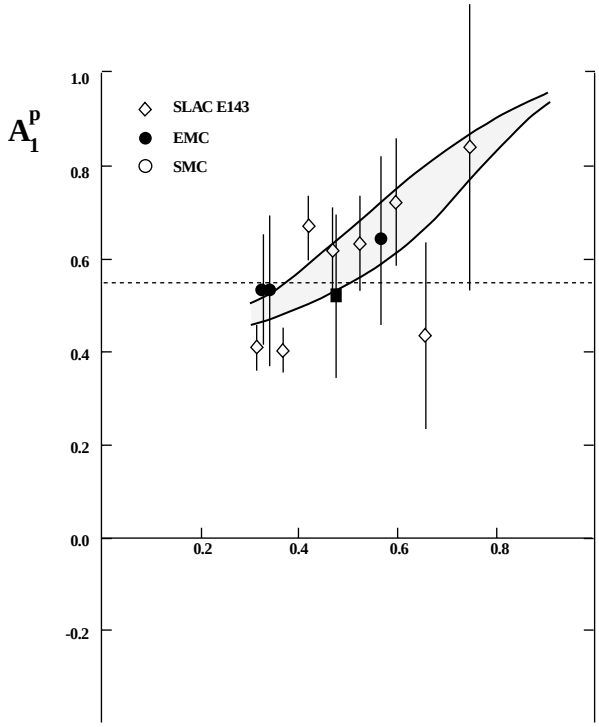

Figure 2: Available DIS A_1^p data in the high x region. The solid band indicates the quark model prediction by Isgur [15].

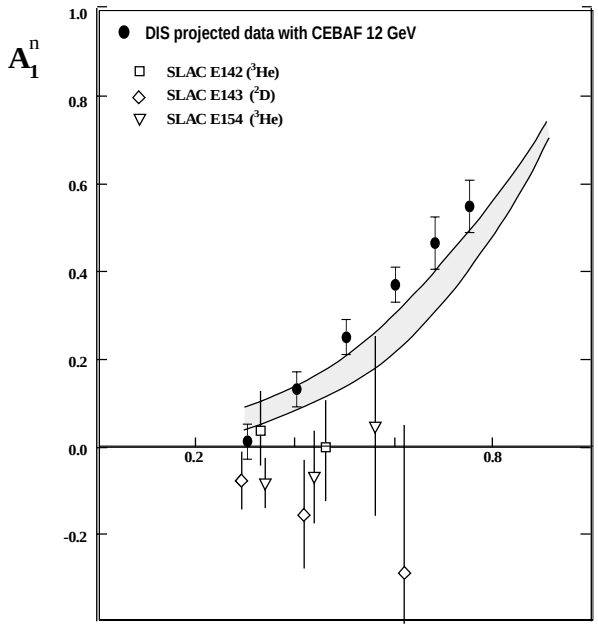

Figure 3: Available DIS A_1^n data in the high x region. The solid circles show the projected DIS data with 12 GeV beam at Jefferson lab. The solid band indicates the quark model prediction by Isgur [15].

2 Spin structure functions in the resonance regions

The exclusive process, $e + p \to e + R$ where R is the final baryon, is described by helicity amplitudes [12]

$$G_m = \frac{1}{2m_N}\langle R, \lambda' = m - \frac{1}{2} \mid \epsilon^{(m)} \cdot j^\mu(0) \mid N, \lambda = \frac{1}{2}\rangle, \tag{1}$$

where $m = \pm 1, 0$, and the polarization vectors are

$$\epsilon^{(\pm)} = (0, \mp 1, -i, 0)/\sqrt{2} \tag{2}$$

$$\epsilon^{(0)} = (\mid q \mid, 0, 0, \nu)/Q \tag{3}$$

For a single sharp resonance R the relation between the spin structure functions and the helicity amplitudes are

$$\left(1 + \frac{Q^2}{\nu^2}\right) g_1 = m_N^2 \delta(W^2 - m_R^2) \left[\mid G_+ \mid^2 - \mid G_- \mid^2 + (-1)^{s_R - 1/2} \eta_R \frac{Q\sqrt{2}}{\nu} G_0^* G_+ \right], \tag{4}$$

$$\left(1 + \frac{Q^2}{\nu^2}\right) g_2 = m_N^2 \delta(W^2 - m_R^2) \left[\mid G_+ \mid^2 - \mid G_- \mid^2 + (-1)^{s_R - 1/2} \eta_R \frac{\nu\sqrt{2}}{Q} G_0^* G_+ \right], \tag{5}$$

where $W^2 = (q + p)^2$, the total hadronic mass squared (p is the momentum of the target nucleon and q is the momentum transfer), and s_R and η_R are the spin and parity of the

resonance. The delta function for the sharp resonance can be approximated by

$$\delta(W^2 - m_R^2) \approx \frac{1}{2m_R} \frac{\Gamma_R/2\pi}{(W - m_R)^2 + \Gamma_R^2/4} \rightarrow \frac{1}{\pi m_R \Gamma_R}. \tag{6}$$

where Γ_R is the width of the resonance.

3 Bloom-Gilman duality and spin structure functions

Recently Carlson and Mukhopadhyay [12] have shown that PQCD arguments lead to duality predictions for spin structure functions measured in DIS and resonance regions. These arguments are summarized in this section.

PQCD counting rules [16] give the high Q^2 behavior of helicity amplitudes as,

$$G_+ = \frac{g_+}{Q^3}, \tag{7}$$

$$G_0 = m_N \frac{g_0}{Q^4}, \tag{8}$$

$$G_- = m_N^2 \frac{g_-}{Q^5}, \tag{9}$$

where $g_{\pm,0}$ are constants. These relationships combined with equations 2-6 yield the high Q^2 behavior of g_1 at the resonance peak,

$$g_1 = \frac{m_N^2}{\pi m_R \Gamma_R} \frac{g_+^2}{Q^6} = \frac{m_N^2}{\pi m_R \Gamma_R} \frac{g_+^2}{(m_R^2 - m_N^2)^3} (1 - x)^3. \tag{10}$$

The second result requires

$$\frac{1}{Q^2} = \frac{1}{W^2 - m_N^2} \frac{1 - x}{x} \approx \frac{1}{(m_R^2 - m_N^2)} (1 - x) \tag{11}$$

for $x \rightarrow 1$ and $W \approx m_R$. Similarly,

$$g_2 = \frac{m_N^2}{\pi m_R \Gamma_R} \frac{(1 - x)^3}{(m_R^2 - m_N^2)^3} g_+ \left(g_+ - \frac{\eta_R (-1)^{s_R - 1/2}}{\sqrt{2}} g_0 \right). \tag{12}$$

In the deep inelastic region g_1 and F_1 are similarly related to quark distributions except for one sign,

$$g_1 = \frac{1}{2} \sum e_q^2 \left[q_\uparrow(x, Q^2) - q_\downarrow(x, Q^2) \right], \tag{13}$$

$$F_1 = \frac{1}{2} \sum e_q^2 \left[q_\uparrow(x, Q^2) + q_\downarrow(x, Q^2) \right], \tag{14}$$

where the $\uparrow$ ($\downarrow$) refers to quark spin parallel (anti-parallel) to the spin of the parent nucleon. PQCD arguments show that $q_\uparrow$ dominates as $x \rightarrow 1$ [17]. Given this condition both

F_1 and g_1 can be expected to behave similarly at high x. Since $F_1 \propto (1-x)^3$ as $x \to 1$ one can expect that

$$\lim_{x \to 1} \quad g_1(x) \propto (1-x)^3 \tag{15}$$

in the DIS region. Equations 10 and 15 show that the x evolution of g_1 is the same in DIS and resonance regions indicating duality for g_1.

The virtual photon asymmetry (A_1) is related to spin structure functions by

$$A_1 \equiv \frac{\sigma_{1/2} - \sigma_{3/2}}{\sigma_{1/2} + \sigma_{3/2}} = \frac{g_1 - \frac{Q^2}{\nu^2} g_2}{F_1}, \tag{16}$$

where $\sigma_{1/2}$ and $\sigma_{3/2}$ are cross sections for photo absorption with total initial state spins of $1/2$ and $3/2$ respectively. For a resonance,

$$A_1 = \frac{\mid G_+ \mid^2 - \mid G_- \mid^2}{\mid G_+ \mid^2 + \mid G_- \mid^2} \tag{17}$$

Since PQCD arguments show that $\mid G_+ \mid \gg \mid G_- \mid$ at high Q^2, A_1 can be expected to go to 1 as $x \to 1$ for the resonance data.

As previously noted there are many different predictions for the high x behavior of A_1^n in the deep inelastic region. SU(6) symmetry breaking quark models and PQCD predict that $A_1^n \to 1$ as $x \to 1$. If this is the case duality can be expected to hold for A_1 as well.

4 Extraction of g_1 and A_1

g_1 and A_1 can be extracted from helicity asymmetry measurements. Longitudinally polarized electrons are scattered from a target that is polarized either longitudinally or transversely to the beam polarization. The longitudinal ($A_\parallel$) and transverse ($A_\perp$) asymmetries are formed by combining data obtained with opposite beam helicity;

$$A_\parallel = \frac{\sigma^{\uparrow\downarrow} - \sigma^{\uparrow\uparrow}}{\sigma^{\uparrow\downarrow} + \sigma^{\uparrow\uparrow}}, \tag{18}$$

$$A_\perp = \frac{\sigma^{\downarrow\rightarrow} - \sigma^{\uparrow\rightarrow}}{\sigma^{\downarrow\rightarrow} + \sigma^{\uparrow\rightarrow}}. \tag{19}$$

The spin structure functions can be extracted from these asymmetries by using,

$$g_1(x,Q^2) = \frac{F_1(x,Q^2)}{d'}[A_\parallel + \tan(\theta/2)A_\perp] \tag{20}$$

$$g_2(x,Q^2) = \frac{yF_1(x,Q^2)}{2d'}\left[\frac{E + E'\cos(\theta)}{E'\sin(\theta)}A_\perp - A_\parallel\right], \tag{21}$$

where E is the beam energy, E' is the scattered electron energy, θ is the scattering angle, $y = (E - E')/E,\ d' = [(1-\epsilon)(2-y)]\,/[y(1+\epsilon R(x,Q^2))],\ \epsilon = 1/(1+2\,[1+\gamma^{-2}]\tan^2(\theta/2), \gamma =$

$2Mx/\sqrt{Q^2}$), M is the nucleon mass and $R(x,Q^2)$ is the ratio of longitudinal to transverse cross sections.

A_1 and A_2 are related to the measured asymmetries by,

$$A_1 = \frac{A_\parallel}{D(1+\eta\zeta)} - \frac{\eta A_\perp}{d(1+\eta\zeta)} \tag{22}$$

$$A_2 = \frac{\zeta A_\parallel}{D(1+\eta\zeta)} + \frac{A_\perp}{d(1+\eta\zeta)} \tag{23}$$

where $D = (1 - E'\epsilon/E)/(1+\epsilon R), \eta = \epsilon\sqrt{Q^2}/(E-E'\epsilon), d = D\sqrt{2\epsilon/(1+\epsilon)}$, and $\zeta = \eta(1+\epsilon)/2\epsilon$.

5 The experiment

We are proposing to measure A_1^{3He} and g_1^{3He} in the resonance region and then use this data to extract A_1^n and g_1^n for the neutron with high precision up to $x = 0.84$. The lower x range ($x < 0.65$) that overlaps with the DIS data from E99-117 can be used to test duality between the resonance and DIS regions for A_1^n and g_1^n. Longitudinally polarized CEBAF beam up to 5.6 GeV will be used with the Hall A polarized ^{3}He high pressure gas target. At beam energies of 3.0 GeV, 4.6 GeV and 5.6 GeV, both Hall A High Resolution spectrometers (HRS) will be used in a symmetric configuration in electron detection mode. A beam current of 15μA combined with a target density of about 1×10^{22} atoms/cm^2 provides a luminosity of about 1×10^{36}cm^{-2}s^{-1} allowing this experiment to be completed in only 23 days.

5.1 The CEBAF polarized beam

In our rate calculations we have assumed 15μA of beam with 80% polarization. Recent Hall A Møller measurements have indicated that beam polarization as high as 79% has been delivered over long periods of time using the strained GaAs source. Thus we believe that by the time this experiment runs, 80% polarization will have been achieved. The beam polarization will be measured with the Hall A Møller and Compton polarimeters.

5.2 The polarized ^{3}He target

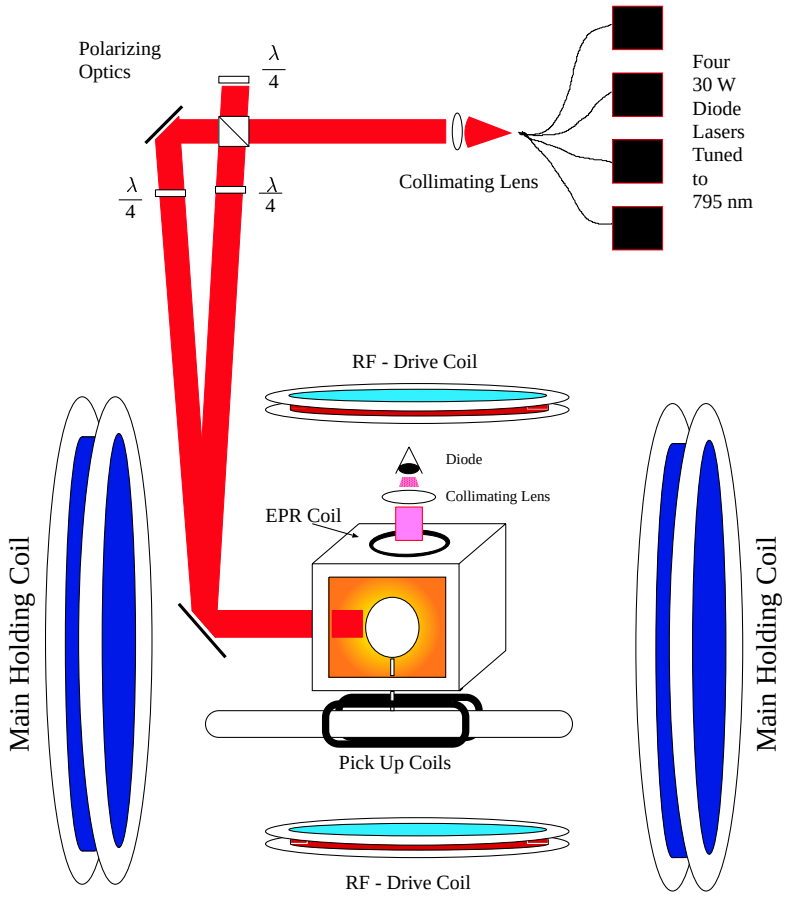

Figure 4: A schematic diagram of the Hall A polarized ^{3}He target

The Hall A polarized ^{3}He target is based on the principal of spin exchange between optically pumped alkali-metal vapor and noble-gas nuclei [22]. This target was successfully used for Jefferson Lab experiments E94-010 and E95-001.

The main feature of the target is the sealed glass cell, which under operating conditions contains ^{3}He at about 10 atmospheres. As shown in Figure 4 the cell consists of two chambers; an upper chamber where the spin exchange takes place and a lower chamber through which the electron beam passes. The appropriate number density of the alkali-metal Rubidium in the upper chamber is maintained by keeping it at a temperature of 170-200°C.

The main coils shown in Figure 4 are large Helmholtz coils used to apply a static magnetic field of about 25 Gauss. Also shown are the components for the NMR and EPR polarimetry. The optics system includes four diode lasers for longitudinal pumping and three for transverse pumping. A polarizing beam splitter lens system and a quarter wave plate are required to condition each laser beam line and provide circular polarization.

5.3 The Spectrometer setup

We plan to use both Hall A High Resolution spectrometers (HRS) in a symmetric configuration in electron detection mode. The spectrometer detector packages will be similar to those to be used for experiment E99-117. Each detector package will consist of:

- A Vertical Drift Chamber (VDC) pair for tracking.
- A pair of trigger scintillator planes.
- Gas Cerenkov counter for pion rejection.
- A lead glass calorimeter for additional pion rejection.

As shown in Figure 5 the worst case e/π ratio for this experiment is about 1:50. Thus the combined pion rejection factor of 2×10^{-4} with Gas Cerenkov and lead glass calorimeter, already achieved by E94-010, is sufficient for this experiment.

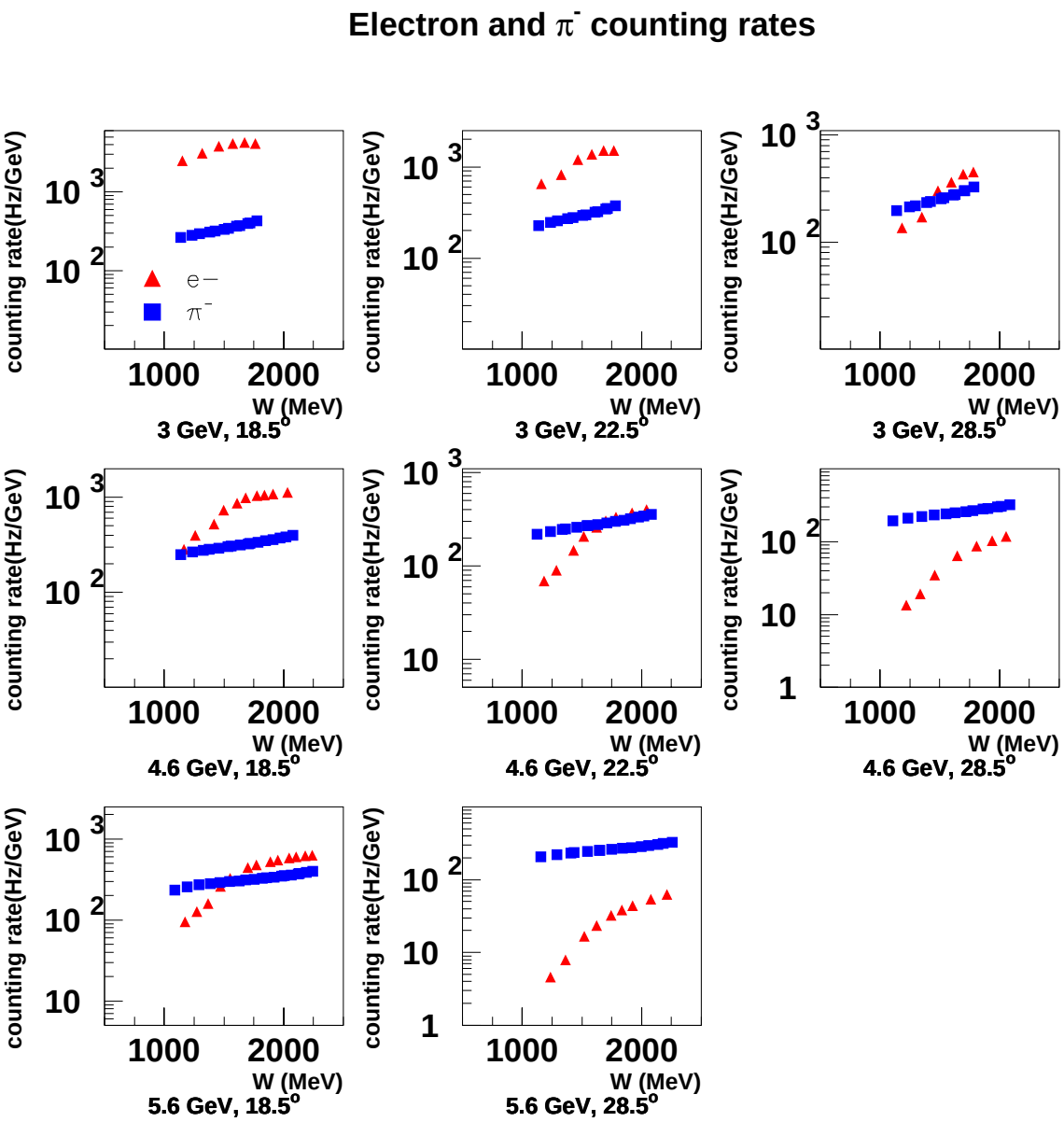

Figure 5: Estimated electron and π^- counting rates.

5.4 Proposed measurement and Data analysis

The measurement consists of collecting $^3\vec{\text{He}}(\vec{e}, e')$ data at scattering angles of 18.5°, 22.5°, and 28.0° with 3.0 GeV and 4.6 GeV beam energies and at 18.5° and 28.5° with 5.6 GeV beam. Each of these settings will consist of six sub settings with different spectrometer momenta to cover the full resonance region.

The raw measured ^{3}He counting asymmetries are converted to the experimental asymme-

try using the relation,

$$A_{\parallel} = \frac{\Delta_{\parallel}}{P_b P_t f} \tag{24}$$

$$A_{\perp} = \frac{\Delta_{\perp}}{P_b P_t f} \tag{25}$$

$$\Delta_{\parallel} = \frac{(N^{\uparrow\downarrow} - N^{\uparrow\uparrow})}{(N^{\uparrow\downarrow} + N^{\uparrow\uparrow})} \tag{26}$$

$$\Delta_{\perp} = \frac{(N^{\downarrow\rightarrow} - N^{\uparrow\rightarrow})}{(N^{\downarrow\rightarrow} + N^{\uparrow\rightarrow})} \tag{27}$$

where $N^{\uparrow\uparrow}$ ($N^{\uparrow\downarrow}$) represents the rate of scattered electrons for each bin in W and Q^2 when the helicity of the incoming electron beam is parallel (anti-parallel) to the target spin. $N^{\downarrow\rightarrow}$ and $N^{\uparrow\rightarrow}$ correspond to the case where the target spin is perpendicular to the beam helicity. $P_b = 0.8$ and $P_t = 0.4$ are the beam and target polarizations respectively. f is the dilution factor that corresponds to the fraction of events that originated from scattering off the neutron in ^{3}He. We will use 40 cm target cells as in experiments 94-010 and 95-001 so that there is little or no dilution of asymmetry due to glass target walls. The excellent position resolution of the HRS pair would allow the removal of target wall events with software cuts. Thus with negligible contamination from glass we expect $f \approx 0.3$.

The systematic uncertainties are dominated by the measurements of beam and target polarizations. To evaluate the systematic uncertainties for the proposed measurement, we used $\Delta P_b/P_b = 0.02$ as presently achieved by the Hall A Møller and Compton polarimeters and $\Delta P_t/P_t = 0.05$, which is the projected uncertainty of E94-010. The systematic uncertainties for the proposed measurement are smaller than or comparable to the statistical uncertainties.

The radiative corrections will be applied in two steps. The external corrections will be evaluated using the Mo and Tsai prescription [20]. The internal corrections will be evaluated and corrected for by using the prescription by Kukhto and Shumeiko [21]. A set of low beam energy (3 GeV) measurements at the same angles as the measurements at the two higher beam energies has been selected especially for use in the radiative corrections of the higher beam energy settings.

5.5 Extraction of neutron information from ^{3}He

In the DIS region, an effective neutron spin structure response can be extracted from that of ^{3}He using the following procedure, where spin contributions from S,S$'$ and D states of ^{3}He are considered [23].

$$\tilde{g_1}^n = \frac{1}{\rho_n}(g_1^{^3He} - 2\rho_p g_1^p) \tag{28}$$

$$\tilde{A_1}^n = \frac{W_1^{^3He}}{W_1^n}\frac{1}{\rho_n}(A_1^{^3He} - 2\frac{W_1^p}{W_1^{^3He}}\rho_p A_1^p) \tag{29}$$

where $\tilde{g_1}^n$, g_1^p and $g_1^{^3He}$ are the spin structure functions for an effective free neutron, a free proton and ^{3}He respectively. The $\tilde{A_1}^n$, A_1^p, $A_1^{^3He}$ terms give the virtual photon asymmetries

for the three particles while W_1^n, W_1^p and $W_1^{^3He}$ give the unpolarized structure functions for the three particles. Because of the pairing of the two protons of ^{3}He mainly in the S state, ^{3}He polarization is dominated by the neutron polarization. $\rho_n = (87 \pm 2)\%$ and $\rho_p = (-2.7 \pm 0.3)\%$ are the polarization values of the neutron and the proton in ^{3}He due to the S, S$'$ and D states of the wave function.

This approach has been shown to work in the DIS region at a few percent level [24]. However, this approach does not include Fermi motion effects or binding effects of the neutron inside ^{3}He. Fermi motion is expected to affect the extraction of the neutron response especially in the resonance region, because of the smearing of the resonance peaks. For the proposed test of duality in this experiment, the important quantity is neither the values of g_1 nor that of A_1 at a certain point of energy transfer but rather the integrated value of these quantities over a resonance region including the contributions from the background [12]. Thus the effects due to Fermi motion will have little effect on the results of this experiment.

A convolution approach to extract the neutron response using a realistic ^{3}He wave function including the full treatment of Fermi motion and binding energy effects has been developed over the last ten years [24]. Currently the development of this method continues especially in the resonance region. Soon this method will be applied to the resonance region spin structure function data from experiment 94-010. This method will also be used by several future polarized ^{3}He experiments in Hall A. Thus, by the time this experiment runs this method will be well tested and we believe that we will be able to use this method to extract the neutron spin response from this experiment at a few percent level.

5.6 Kinematics and rate estimates

Tables 1-3 give the kinematics, electron rates and expected uncertainties. For the rate calculations we have assumed a beam current of 15 μA, the combined angular acceptance of the HRS pair (2×6 msr) and the flat region of the HRS momentum acceptance ($\pm$ 4%). 15μA of beam combined with a target density of about 1×10^{22} atoms/cm^2 provides a luminosity of about 1×10^{36}cm^{-2}s^{-1}. The cross sections were calculated by using the code QFS [25] of Lightbody and O'Connell.

E_0 (GeV)	θ_e (degrees)	E' (GeV)	Q^2 $(GeV)^2$	$\bar{W}$ (GeV)	$\bar{x}$	Rate Hz	ΔA_1^n	Time Hours
3.0	18.5	2.5	0.77	1.18	0.52	297	0.02	5
		2.3	0.71	1.34	0.43	375	0.02	3
		2.1	0.65	1.46	0.33	457	0.02	3
		1.8	0.56	1.57	0.27	497	0.02	2
		1.6	0.51	1.67	0.22	509	0.02	2
		1.9	0.60	1.75	0.18	490	0.02	2
3.0	22.5	2.3	1.05	1.19	0.66	79	0.03	5
		2.1	0.98	1.34	0.50	98	0.03	4
		1.9	0.90	1.47	0.40	145	0.03	3
		1.7	0.77	1.57	0.33	182	0.03	2
		1.6	0.71	1.67	0.28	180	0.03	2
		1.8	0.83	1.75	0.24	164	0.03	2
3.0	28.5	2.1	1.50	1.19	0.73	16	0.04	28
		1.9	1.38	1.34	0.59	21	0.04	13
		1.7	1.28	1.47	0.49	36	0.04	4
		1.6	1.18	1.57	0.41	43	0.04	3
		1.5	1.10	1.67	0.36	52	0.04	2
		1.4	1.00	1.75	0.31	54	0.04	2

Table 1: Kinematics, rates and statistical uncertainties for the proposed 3 GeV measurements. A 100 MeV momentum bin has been used for the rate calculations. Due to the HRS momentum acceptance of $\sim \pm 4\%$, each momentum setting considered here contains 2-3 100 MeV bins. The rates and the uncertainties given are for the bin with the lowest rate of a given momentum setting.

E_0 (GeV)	θ_e (degrees)	E' (GeV)	Q^2 $(GeV)^2$	$\bar{W}$ (GeV)	$\bar{x}$	Rate Hz	ΔA_1^n	Time Hours
4.6	18.5	3.6	1.70	1.23	0.72	34	0.04	10
		3.3	1.57	1.46	0.55	62	0.04	5
		3.0	1.44	1.63	0.44	104	0.04	3
		2.8	1.34	1.78	0.36	251	0.04	2
		2.6	1.23	1.94	0.29	129	0.04	2
		2.4	1.14	2.05	0.24	134	0.03	2
4.6	22.5	3.2	2.28	1.23	0.76	8	0.05	17
		3.0	2.10	1.46	0.62	18	0.05	7
		2.8	1.94	1.63	0.51	31	0.05	4
		2.6	1.79	1.78	0.41	39	0.05	3
		2.4	1.65	1.94	0.35	44	0.05	2
		2.2	1.53	2.05	0.30	48	0.05	2
4.6	28.5	2.8	3.11	1.23	0.82	1.6	0.06	38
		2.6	2.87	1.46	0.66	4.1	0.06	14
		2.4	2.65	1.63	0.56	7.6	0.06	7
		2.2	2.44	1.78	0.49	10.	0.06	5
		2.0	2.25	1.94	0.43	12.	0.06	3
		1.8	2.10	2.05	0.37	14.	0.06	3

Table 2: Same as in Table I but for =4.6 GeV beam energy. For the settings with $E' < 3$ GeV, the combined solid angle of the HRS pair (12 msr) was used. However for the settings with $E' > 3$ GeV only the HRSE solid angle was used since HRSH is not operable above 3.1 GeV.

E_0 (GeV)	θ_e (degrees)	E' (GeV)	Q^2 $(GeV)^2$	W (GeV)	$\bar{x}$	Rate Hz	ΔA_1^n	Time Hours
5.6	18.5	4.2	2.42	1.24	0.78	11	0.06	24
		3.8	2.33	1.55	0.58	31	0.06	8
		3.6	2.10	1.75	0.47	53	0.06	4
		3.3	1.90	1.92	0.39	63	0.06	3
		2.8	1.75	2.06	0.33	70	0.06	2
		3.3	1.62	2.22	0.29	75	0.06	2
5.6	28.5	3.1	4.27	1.24	0.84	0.7	0.06	105
		2.9	3.90	1.55	0.72	2.5	0.06	27
		2.6	3.50	1.75	0.62	4.7	0.06	13
		2.4	3.23	1.92	0.52	5.4	0.06	9
		2.3	3.10	2.06	0.45	6.5	0.06	7
		2.1	2.87	2.22	0.40	7.5	0.06	5

Table 3: Same as in Table I but for =5.6 GeV beam energy. For the settings with $E' < 3$ GeV, the combined solid angle of the HRS pair (12 msr) was used. However for the settings with $E' > 3$ GeV only the HRSE solid angle was used since HRSH is not operable above 3.1 GeV.

The Q^2/W phase-space covered by this experiment is given in Figure 6. Figure 7 shows the expected data for the three resonance regions compared to the available world data and

projected E99-117 data.

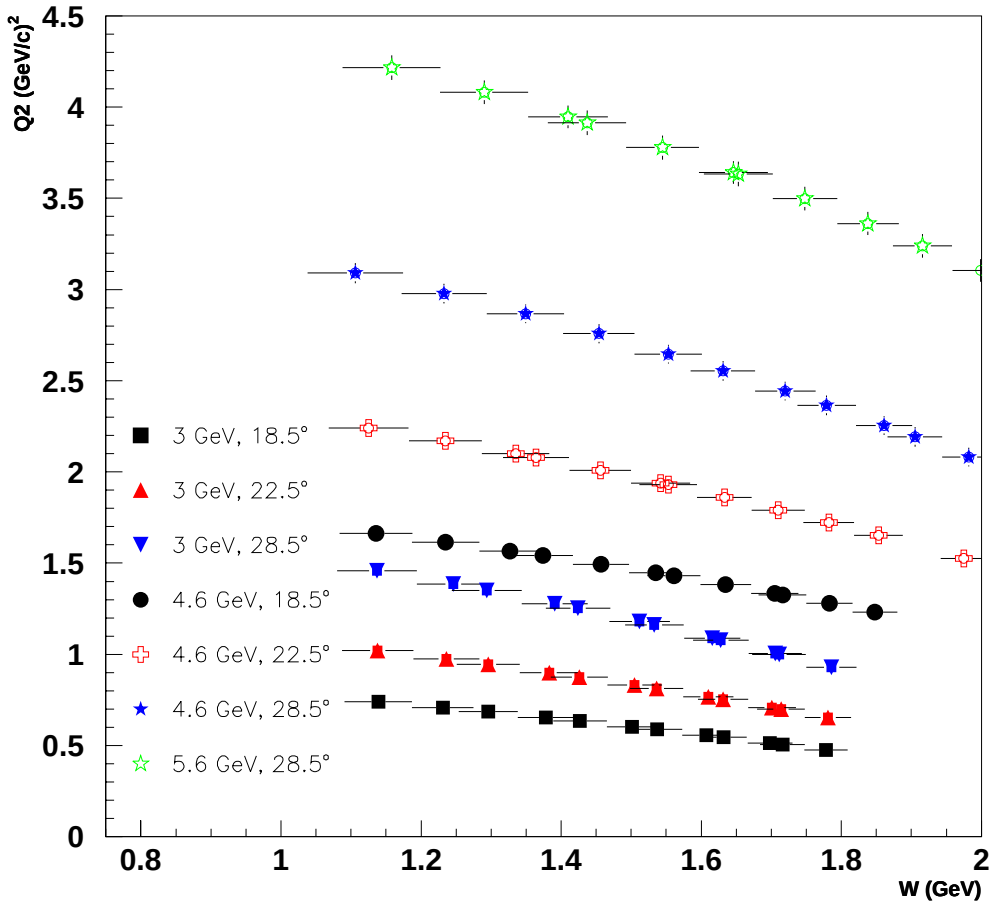

Figure 6: The proposed Q^2 and W coverage

The total measurement time as given in tables 1-3 is 425 hours. This beam time allows for almost complete coverage of the resonance region in Q^2 ($0.8 < Q^2 < 4.2$ (GeV/c)^2), in x ($0.5 < x < 0.85$), and in W ($1.0 < W < 2.2$ GeV). In addition to this time 50 hours for momentum changes, 10 hours for angle changes, 8 hours for four Møller measurements, 16 hours for beam energy changes, 9 hours for beam energy measurements and 24 hours for calibration will be required.

6 Summary and Request

In summary, we propose a precision measurement of the spin structure function g_1^n and the virtual photon asymmetry A_1^n of the neutron in the resonance region up to $Q^2 = 4.2$ (GeV/c)^2. For the Δ resonance this covers the x range up to $x = 0.84$. For $x < 0.65$ resonance data from this experiment and DIS data from E99-117 overlap enabling a precision test of duality predictions for spin structure functions. When 12 GeV beam becomes available at Jefferson Lab, the DIS measurements could be extended to $x \approx 0.75$, These high x DIS data

combined with the data from this proposed measurement will provide a complete test of duality up to $Q^2 = 8$ (GeV/c)^2 and $x = 0.75$. The demonstration of quark-hadron duality for spin structure functions will enable the use of resonance data as a very powerful tool to study the very high x range ($0.8 < x < 0.95$).

The proposed measurement requires 425 hours of data taking along with 50 hours for momentum changes, 10 hours for angle changes, 8 hours for four Møller measurements, 16 hours for the beam energy changes, 9 hours for beam energy measurements and 24 hours for calibration. We therefore request a total of 542 hours (23 days) of beam time.

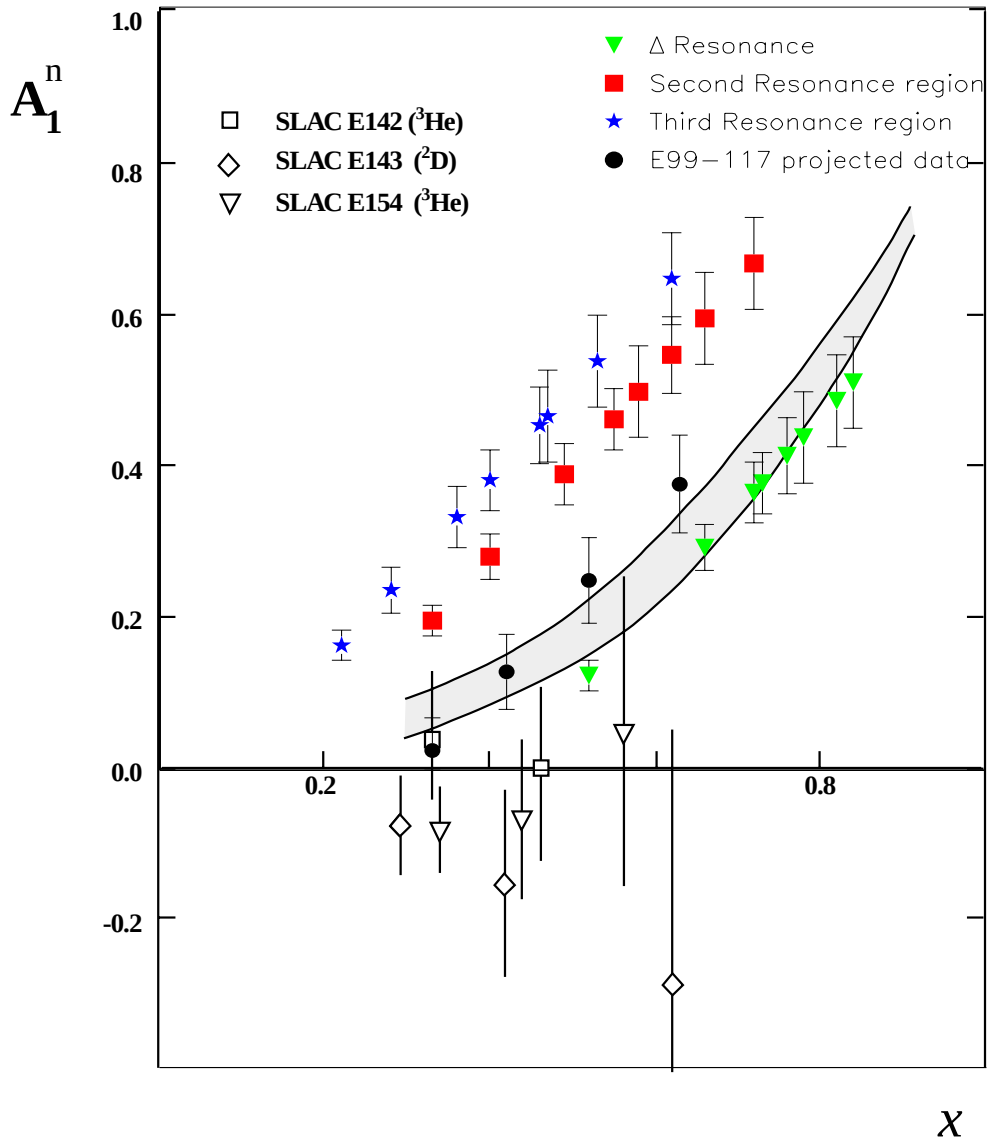

Figure 7: The projected data for the proposed measurement in the three resonance regions. Note that the values of A_1^n for the three resonance regions have been shifted by different offsets to ensure clarity. The solid circles show the projected data for E99-117

References

[1] Particle Data Group, *Review of Particle Physics* Eur. Phys. J. **C3**, p. 199 (1998)

[2] K. Abe *et al.*, phys. Rev. Lett. **78**, 815 (1997).

[3] Jefferson Lab experiment 94-010, Z. E. Meziani, G. Cates and J. P. Chen spokespersons.

[4] Jefferson Lab experiment 93-009, S. E. Kuhn spokesperson; Jefferson Lab experiment 96-002, Oscar A. Rondon spokesperson.

[5] Jefferson Lab experiment 99-117, Z. E. Meziani, J. P. Chen, P. Souder spokespersons.

[6] E. D. Bloom and F. J. Gilman, Phys. Rev. Lett. **25**, 1140 (1970); Phys. Rev. **D 4**, 2901 (1971).

[7] De Rujula, H Georgi, and H. D. Politzer, Ann. Phys. (N.Y.) **103** 315(1977).

[8] C. E. Carlson and N. C. Mukhopadhyay, Phys. Rev. **D 41**, R2343 (1990); Phys. Rev. **D 47**, R1737 (1993); Phys. Rev. Lett. **74**, 1228 (1995).

[9] X. Ji and P. Unrau, Phys. Rev. **D 52**, 72 (1995).

[10] X. Ji and Melnitchouk, Phys. Rev. **D 56**, 1 (1997).

[11] M. Niculescu *et al.*, Phys. Rev. Lett. (2000), to be published; M. Niculescu, PhD Thesis, Hampton University, (unpublished)

[12] C. E. Carlson and N. C. Mukhopadhyay, Phys. Rev. **D 58**, 094029 (1998).

[13] F. Close, Phys. Lett. **B43**, 422 (1973), Nucl. Phys. **B80**, 269 (1974); and *An Introduction to Quarks and Partons*, Academic Press, N.Y., p. 197 (1976)

[14] R. Carlitz, Phys. Lett. **B58** 345 (1975)

[15] N. Isgur, Phys. Rev. **D 59**, 034013 (1999).

[16] S. J. Brodsky and G. R. Farrar, Phys. Rev. Lett. **31**, 1153 (1973); Phys. Rev. **D 11**, 1309 (1975).

[17] G. R. Farrar and D. R. Jackson, Phys. Rev. Lett. **35**, 1416 (1975).

[18] N. Kochelev, Phys. Rev. **D57**5539 (1998); N. Kochelev and A. De Roeck hep-ph/9803330

[19] S. Wandzura and F. Wilczek, Phys. Lett. **B72**, 195 (1977).

[20] L. W. Mo and Y. S. Tsai, Rev. Mod. Phys. **41**, 205 (1969).

[21] T. V. Kukhto and N. M. Shumeiko, Nucl. Phys. **B219** 412 (1983); I. V. Akushevich and N. M. Shumeiko, Nucl. Part. Phys. **20** 513 (1994).

[22] N. R. Newbury, A. S. Barton, P. Bogoard, G. D. Cates, M. Gatzke, H. Mabuchi and B. Saam, Phys. Rev. **A 48** 558 (1993).

[23] J. L Friar *et al.*, Phys. Rev. **C 42**, 2310 (1990).

[24] C. Ciofi delgi Atti, S. Scopetta, E. Pace, G. Salme, Phys. Rev. **C 48**, R969 (1993); C. Ciofi delgi Atti, S. Scopetta, Phys. Lett. **B404**, 223 (1997).

[25] J. W. Lightbody Jr. and J. S. O'Connell, Computers in Physics, 1988.